Published in final edited form as:
Arch Biochem Biophys. 2013 July 1; 535(1): . doi:10.1016/j.abb.2013.02.006.

Structural and Functional Consequences of Cardiac Troponin C L57Q and I61Q Ca^{2+}-Desensitizing Variants

Dan Wang[1], **Michelle E. McCully**[1,2], **Zhaoxiong Luo**[1], **Jonathan McMichael**[1], **An-Yue Tu**[1], **Valerie Daggett**[1,2], and **Michael Regnier**[1,3,*]

[1]Department of Bioengineering, University of Washington, Seattle, Washington, WA 98195, USA

[2]Biomolecular Structure and Design Program, University of Washington, Seattle, Washington, WA 98195, USA

[3]Center for Cardiovascular Biology, University of Washington, Seattle Washington, WA 98109, USA

Abstract

Two cTnC variants, L57Q and I61Q, both of which are located on helix C within the N domain of cTnC, were originally reported in the skeletal muscle system [Tikunova and Davis (2004) *J Biol Chem 279*, 35341-35352], as the analogous L58Q and I62Q sTnC, and demonstrated a decreased Ca^{2+} binding affinity. Here, we provide detailed characterization of structure-function relationships for these two cTnC variants, to determine if they behave differently in the cardiac system and as a framework for determining similarities and differences with other cTnC mutations that have been associated with DCM. We have used an integrative approach to study the structure and function of these cTnC variants both in solution and *in silico*, to understand how the L57Q and I61Q mutations influence Ca^{2+} binding at site II, the subsequent effects on the interaction with cTnI, and the structural changes which are associated with these changes. Steady-state and stopped flow fluorescence spectroscopy confirmed that a decrease in Ca^{2+} affinity for recombinant cTnC and cTn complexes containing the L57Q or I61Q variants. The L57Q variant was intermediate between WT and I61Q cTnC and also did not significantly alter cTnC-cTnI interaction in the absence of Ca^{2+}, but did decrease the interaction in the presence of Ca^{2+}. In contrast, I61Q decreased the cTnC-cTnI interaction in both the absence and presence of Ca^{2+}. This difference in the absence of Ca^{2+} suggests a greater structural change in cNTnC may occur with the I61Q mutation than the L57Q mutation. MD simulations revealed that the decreased Ca^{2+} binding induced by I61Q may result from destabilization of the Ca^{2+} binding site through interruption of intra-molecular interactions when residue 61 forms new hydrogen bonds with G70 on the Ca^{2+} binding loop. The experimentally observed interruption of the cTnC-cTnI interaction caused by L57Q or I61Q is due to the disruption of key hydrophobic interactions between helices B and C in cNTnC. This study provides a molecular basis of how single mutations in the C helix of cTnC can reduce Ca^{2+} binding affinity and cTnC-cTnI interaction, which may provide useful insights for a better understanding of cardiomyopathies and future gene-based therapies.

*Corresponding author: Phone: +1 206 6161 4325, Fax: +1 206 685 3300, mregnier@u.washington.edu.

Keywords

Troponin C; Troponin I; Calcium binding; Fluorescence spectroscopy; Molecular dynamic simulation

INTRODUCTION

Cardiac muscle contraction is tightly controlled by the influx and efflux of Ca^{2+} from the cytosol of cardiomyocytes. Contraction is initiated by Ca2+ binding to cardiac troponin C (cTnC), a member of the EF-hand protein family and the Ca^{2+}-binding subunit of cardiac troponin (cTn). Ca^{2+} binding to the site II of the N-terminal of cTnC (cNTnC) initiates thin filament activation in cardiac muscle, subsequent to force generation and contraction (for reviews, see (1, 2)). In the presence of Ca^{2+} the switch region of cTnI (from residues 147-163) interacts with cNTnC, resulting in reduced interaction of the inhibitory region of cTnI with actin. This allows increased mobility of tropomyosin (Tm), with subsequent exposure ofs myosin binding sites on actin, allowing crossbridge formation to ultimately generate force (1, 3).

In recent years, numerous mutations in human cTnC and other cTn subunits have been identified as associated with cardiomyopathies (4, 5). Functional studies of Dilated Cardiomyopathy (DCM) mutations in thin filament regulatory proteins generally demonstrate a decrease in the Ca^{2+} sensitivity of force development (6-8), suggesting a correlation between Ca^{2+} desensitization of the cardiac myofilament and the pathogenesis of DCM. Recently, Lim *et al* (2008) reported that expression of DCM associated mutation cTnC (E59D, D75Y) in isolated rat cardiomyocytes induced a significant reduction in contractility and led to impaired myofilament Ca^{2+} responsiveness in permeabilized cardiomyocytes (6). However, these fundamentally functional changes at the level of the sarcomere may not be the disasease causing agent itself, and could be associated with the progression and severity of these diseases over time. Moreover, there are relatively few mutations in cTnC that have been found in patients, and there is a lack of scientific knowledge on how rare mutations might lead to cardiac muscle dysfunction.

Others (9-12) and we (13) have been using site-directed mutagenesis of recombinant cTnC to develop and study how they affect troponin function and the regulation of contractile properties of cardiac myofilaments. In this study we have focused on two cTnC variants, L57Q and I61Q, both of which are located on helix C within the N domain of cTnC to determine how they affect the molecular level structure of cTnC, it's interaction with the switch peptide of cTnI, and the correlative functional changes of these two proteins. While neither L57Q nor I61Q cTnC has been identified in patients, detailed characterization of structure-function relationship can provide a framework for determining similarities and differences with other cTnC mutations, especially those that have been identified as associated with DCM, such as cTnC (E59D, D75Y) (6). Additionally, the effects of L57Q and I61Q cTnC were originally reported for the skeletal muscle system (10, 11), as the analogous L58Q and I62Q skeletal TnC (sTnC), and demonstrated a decreased Ca^{2+} binding affinity. Thus studying these cTnC variants can also be instructive to how the structure and function of troponin differs in cardiac vs. skeletal muscle. In the heart, Parvatiyar *et al.* (14) found that I61Q cTnC decreased both Ca^{2+} sensitivity of skinned porcine papillary contraction and ATPase sensitivity, while L57Q showed a substantial decrease in the Ca^{2+} sensitivity of myofilament contraction. We have confirmed that I61Q cTnC reduces the Ca^{2+} sensitivity of force development, and reported that it also slows the rate of thin filament activation, making it the limiting process in force development of myofibrils, while having no effect on maximal relaxation kinetics (15).

While the consequences of these, and other cTnC mutations, have begun to be characterized in terms of their effect on mechanical performance of cardiac muscle, the protein structure-function changes that underlie these effects on contractile properties are not known. To understand how the L57Q and I61Q variants influence Ca^{2+} binding at site II, the subsequent effects on the interaction with cTnI, and the structural changes which are associated with these changes, we have used an integrative approach to study the structure and function of cTnC both in solution and *in silico*. We coupled biochemical experiments and all-atom explicit solvent molecular dynamics (MD) simulations to probe the relationship between molecular structure, movement, and function. Steady-state and stopped flow fluorescence spectroscopy confirmed that a decrease in Ca^{2+} affinity for recombinant cTnC and cTn complexes containing the L57Q or I61Q variants, and the binding of cTnI to cTnC was also reduced. MD simulations of protein constructs containing the regulatory domain of cTnC (cNTnC) in the Ca^{2+} saturated state complexed with the switch region of cTnI (residues 147-163) suggest that I61Q disrupted the key hydrophobic interactions between helices B and C in cNTnC and formed new interactions with the residues on the Ca^{2+} binding loop, which in turn decreased cTnI and Ca^{2+} binding to cNTnC.

MATERIALS and METHODS

Protein Mutagenesis and Purification

Wild-type rat cTnC, cTnI and cTnT in pET24a vector was constructed and expressed as described previously (16). $cTnC^{C35S}$, $cTnC(L57Q)^{C35S}$ and $cTnC(I61Q)^{C35S}$ were constructed from the rat wild-type cTnC plasmid using a primer based Site-Directed Mutagenesis Kit. The mutations were confirmed by DNA sequence analysis. The plasmids for cTnC variants were transformed into *E.coli* BL21 cells and expressed and purified. The L57Q and I61Q variants were engineered using a quikchange site-directed mutagenesis kit from stratagene (using paired 30-mer oligonucleotides, 5′-AAG GTG ATG AGA ATG CAA GGC CAG AAC CCC-3′ and 5′-GGG GTT CTG GCC TTG CAT TCT CAT CAC CTT-3′).

Fluorescent Labeling

$CTnC^{C35S}$ and other variants were labeled with the environmentally sensitive fluorescence probe IANBD at C84 of cTnC as previous described (17). We have demonstrated that the fluorescence probe at C84 of cTnC monitors the N-terminal Ca^{2+} binding of cTnC(17). Labeling efficiency and protein concentration were determined as described previously (13)

Reconstitution of Tn Complexes—The cTn complexes were reconstituted as described (13, 18). The cTn subunits all contained recombinant rat cardiac cTnI, cTnT and $cTnC^{C35S}$ or cTnC variants.

Steady-state Fluorescence Measurements

All steady-state fluorescence measurements were performed using a Perkin Elmer Luminescence Spectrometer LS50B at 15°C. IANBD fluorescence was excited at 490nm and monitored at ~530 nm with bandwidths set at ~8nm. Small, progressive amount of Ca^{2+} or cTnI were titrated into cTnC or cTn complex (0.6μM) in 20mM MOPS, 150mM KCl, 3mM $MgCl_2$, 2mM EGTA, 1mM DTT (pH 7.0), same as previously described (19). Upon binding to Ca^{2+} or cTnI in the presence (100 μM) or absence of Ca^{2+}, the change of the hydrophobicity or polarity of the environment were detected by the IANBD probe, in this case, giving an increased fluorescence signal. The free Ca^{2+} concentration was calculated by the Maxchelator program (http://maxchelator.stanford.edu) (20). The Ca^{2+} dependence of conformational changes (reported as the pCa value at half maximal fluorescent signal change) and the dissociation constant K_D of cTnI for cTnC were obtained by fitting the binding data with the Hill equation.(21). The results represent the mean ± S.E.M of three to

five successive titrations. Statistical significance was determined by Student's t-test using SigmaPlot Software Package (Systat SoftwareInc.). $p < 0.05$ was considered as statistical significance.

Stopped-Flow Fluorescent Measurements

Ca^{2+} dissociation rate (k*off*) from whole cTn (containing WT or cTnC variants) and reconstituted thin filaments was measured at 15 °C using an Applied Photophysics Ltd. model SX-18MV stopped-flow instrument (Leatherhead, U.K.) as previously described (9, 11, 22). k*off* from whole cTn was measured by rapidly mixing the protein with the fluorescent Ca^{2+} chelator Quin-2 (Calbiochem) excited at 330 nm and monitored emission through a 510 nm broad bandpass interference filter (Oriel). The solution buffer used for the measurements was 10 mM MOPS, 150 mM KCl, 1 mM DTT, 3 mM $MgCl_2$, at pH 7.0. 10 mM EGTA was utilized to remove 200 μM Ca^{2+} from the Tn complexes or thin filaments. Data traces (an average of 3 individual traces) were fit with a single exponential equation to calculate the kinetic rates.

MD Simulations and Analysis

All-atom, explicit solvent molecular dynamics (MD) simulations were performed at 288 K and neutral pH in the micro canonical (NVE, constant number of particles, volume, and energy) ensemble using the *in lucem* molecular mechanics (*il*mm) program (23) with the Levitt *et al.* (24) force field. The starting structure of the N-terminus of wild type cTnC (cNTnC, residues 1 to 89) bound to $cTnI_{147\text{-}163}$ complex was taken from model 18 of the NMR structure (PDB entry 1mxl) (25). The L57Q and I61Q single mutations were created manually using UCSF Chimera (26). The starting structures were minimized for 1000 steps using steepest descent minimization,and then solvated in a rectangular box of flexible three-center (F3C) waters (27) with walls located at least 10 Å from any protein atom. The solvent density of the box was set to 0.999129 g/mL, the experimental value for 288K (28) which was set as the simulation temperature. A 2 fs time step was used, and structures were saved every 1 ps. Multiple ($n \geq 3$) simulations for the $cTnI_{147\text{-}163}$•cNTnC•Ca^{2+} complexes (L57Q, I61Q and WT), were performed for 70ns each. All protein images were generated using UCSF Chimera.

Analysis of the MD trajectories was performed with *il*mm as described previously (17). The root-mean-square deviations (RMSD) of the Cα atoms to the NMR structure were calculated to measure the degree of structural change from the starting conformation. Contacts between residues were identified where the distance between two carbon atoms was ≤ 5.4 Å or any other non-carbon atoms were ≤ 4.6 Å. These contacts were further classified as intra- and inter-molecular hydrogen bonds, hydrophobic contacts and other non-specific interactions. A hydrogen bond was defined if the distance between the acceptor-donor was ≤ 2.6 Å and donor-hydrogen-acceptor angle was > 135°. Hydrophobic contacts were identified when the carbon-carbon distance was ≤ 5.4 Å. Any two non-carbon (and non-hydrogen) atoms were considered to make a non-specific interaction when ≤ 4.6 apart. The distances between the center of mass (COMdist) of helices B/C were calculated as the distances between the centers of mass of the two groups of residues in helices B (residues 41-48) and C (residues 54-64). The Cα RMSD of helices B/C to the starting structure was also monitored over time to detect any structural alterations. D65, D67, S69, T71, D73, and E76 were considered to be the Ca^{2+} binding coordinating residues and are located in the regulatory domain of cTnC. The interaction of these residues with each other and the Ca^{2+} binding pocket itself are critical regulators of the contractile process. Residue 61 is located very close to the Ca^{2+} pocket, and thus contacts formed between residue 61 and residues in the Ca^{2+} binding loop were probed to address any disruption at this site due to the I61Q mutation.

RESULTS and DISCUSSION

Effects of cTnC (L57Q) and cTnC (I61Q) variants on the binding of Ca^{2+} to cTn complexes

We have shown previously that trabeculae exchanged with cTn containing recombinant cTnC (I61Q) (161Q cTn) have reduced Ca^{2+} sensitivity of contraction (pCa_{50}) and thin filament activation kinetics (15). Trabeculae exchanged with L57Q cTn also have decreased Ca^{2+} sensitivity of force compared to WT cTn (unpublished data). To explore the molecular mechanism of how these single amino acid substitutions in cTnC affect cTn function that regulates the contractile properties of cardiac muscle, here we focus on the interaction between these two cTnC variants with their two ligands, Ca^{2+} and cTnI.

To investigate Ca^{2+} binding affinity to cTn complexes containing the cTnC variants using steady state fluorescence spectroscopy, a C35S mutation was introduced, allowing site specific labeling at Cysteine 84 of cTnC with the hydrophobicity-sensitive fluorescence probe IANBD. Figure 1 shows representative wavelength scans for 0.6 μM cTnC alone (blue trace) and the increase in fluorescence with addition of Ca^{2+} (red trace). This indicates that Ca^{2+} binding induces a conformational change in cNTnC that leads to increased hydrophobicity of the environment around the IANBD-labeled cysteine. To confirm this, we also tested D65A $_{\mathrm{IANBD}}$, which disrupts Ca^{2+} binding at site II of cTnC(29). Not surprisingly, the fluorescence signal decreased upon addition of Ca^{2+}, due to the dilution of the concentration of fluoro-probe in the system (data not shown). Thus, a n increase in IANBD fluorescence is associated with the increased binding of Ca^{2+} to cTnC.

The total magnitude of fluorescence signal increase was significantly less for isolated $_{\mathrm{IANBD}}$ compared to the control $_{\mathrm{IANBD}}$, ~1.15 fold (for I61Q) *vs*. ~1.25 fold (for control), as shown in the inset graph of Figure 2. cTnC (L57Q) also had a slightly lower increase in fluorescence (~1.21 fold) compared with control. These results suggest the regulatory domain of $_{\mathrm{IANBD}}$ underwent smaller conformational changes for the cTnC (I61Q) and cTnC (L57Q) variants, suggesting less exposure of hydrophobic residues (which can interact with the cTnI switch peptide) compared to control cTnC.

The Ca^{2+} binding affinities of cTn complexes were determined from the data in Figure 2, and are reported as the pCa that elicited half-maximal increase in fluorescence (pCa_{50}). L57Q and I61Q decreased Ca^{2+} binding affinity, as indicated by reduction of pCa_{50} by ~0.28 and ~0.84 pCa units, respectively (pCa 6.58±0.01 for L57Q $_{\mathrm{IANBD}}$ and 6.15 ±0.01 for I61Q $_{\mathrm{IANBD}}$). Similar results were reported for analogous positional mutations of L58Q and I62Q cTnC in skeletal TnC by Tikunova and Davis *et al.* using steady-state fluorescence measurements with a different labeling system. They reported decreased Ca^{2+} binding affinity in both of the variants, but especially for sTnC (I62Q), with a dramatic decrease of ~0.9 pCa units, shifting the pCa_{50} to the right (10).

Effects of cTnC (L57Q) on Ca^{2+} dissociation rates

The Ca^{2+} dissociation rate (k_{off}) of whole cTn (with WT cTnI, cTnT) and the thin filament (with cTn, actin and cTm) was determined with stopped-flow fluorimetry using Quin-2 as a reporter for free Ca^{2+}. We have previously reported the k_{off} for I61Q cTnC (15). Table 1 summarizes the results for L57Q compared to WT and I61Q. In both cTn and thin filament studies, k_{off} was faster for I61Q than WT cTn, as well as any other variants that have been tested. k_{off} for L57Q was faster than WT but not as fast as I61Q cTn. The relative order of increasing k_{off} was maintained for measurements of recombined thin filaments, but the rates were all faster compared to cTn alone. This is consistent with previous reports from Davis and Tikunova (10, 11) for analogous mutations in sTnC. Moreover, disease-related cardiac

contractile protein mutations have been shown to change the rate of Ca^{2+} dissociation from TnC (30, 31).

Effects of cTnC(L57Q) and cTnC(I61Q) variants on cTnC-cTnI interaction

A critical step in activation of thin filaments and contraction is the increase in cTnC-cTnI interaction that occurs following Ca^{2+} binding to cTnC. To study the affinity of the cTnC variants for cTnI, IANBD-labelled cTnC was titrated with cTnI in the presence and absence of Ca^{2+}. As shown in Figure 3A, I61Q cTnC had reduced interactions with cTnI in both apo (K_D=328±22nM) and Ca^{2+} saturated states (K_D=241±12nM). In contrast, L57Q cTnC was similar to WT cTnC in the apo state (K_D=271±17nM), suggesting a similar starting (apo) structure as for WT cTnC. However, in the Ca^{2+} saturated states the affinity of cTnI for L57Q cTnC (K_D=228±9nM) was reduced to a similar level as I61Q (Figure 3B). The magnitude of the maximal fluorescence also changed, control > L57Q >I61Q cTnC, indicating that the exposure of the hydrophobic patch within cNTnC might be disrupted by L57Q and I61Q. Interestingly, we recently reported that the L48Q cTnC variant, which has increased Ca^{2+} binding affinity and a slower Ca^{2+} k_{off}, resulted in increased cTnC-cTnI interaction in both the apo and Ca^{2+} saturated states (13) and resulted an increased Ca^{2+} sensitivity of contraction (15). Combined, these data suggest the apo state my provide a better prediction of the ability of cTnC variants to activate cardiac thin filaments and regulate the Ca^{2+} sensitivity of contraction.

MD simulations

To investigate the structural changes that may explain the experimental observed effects on Ca^{2+} and cTnI binding to cTnC, multiple (n≥3) independent MD simulations at neutral pH and 15 °C were performed for WT, L57Q and I61Q cNTnC•Ca^{2+}•$cTnI_{147\text{-}136}$ complexes (70ns each). After the initial equilibration period, the Cα RMSDs generally reached a plateau at ~4 Å (WT 4.2±0.2 Å, L57Q 3.9±0.6 Å, and I61Q 4.1±0.7 Å), suggesting that all systems were stable.

The MD simulations with the chosen fragments of the cTnI-cTnC complex allow for the visualization of interactions between the mutated residue and the rest of the structure, as well changes in conformation that may result in altered cTnI-cTnC interaction. Residue L57 and I61 are both on helix C with 61 closer to the Ca^{2+} binding site and 57 nearer to helix B (Figure 4).

Effects of cTnC (I61Q) and cTnC(L57Q) substitution on the mobility of helix B and C in cNTnC

In simulations of the I61Q cNTnC•Ca^{2+}•$cTnI_{147\text{-}136}$ complex helices B and C moved apart, as shown in Figure 5 (For movies, see supplementary material). This movement did not occur for any of the WT cNTnC•Ca^{2+}•$cTnI_{147\text{-}136}$ complex simulations nor in any of L57Q simulations, suggesting the I61 position has more influence on the mobility of helices B and C. For all simulations there were no significant differences in movement of these helices for L57Q vs. WT cTnC. Interestingly, the movement between helices B and C for I61Q was very different from what was observed in a previous study of cTnC(L48Q), where movement of helix B away from the rest of the protein facilitated the exposure of the hydrophobic patch and stabilized the open state of cNTnC (19).

To quantify helical movements in the I61Q cNTnC•Ca^{2+}•$cTnI_{147\text{-}136}$ simulations and compare with WT as well as the L57Q cTnC variant simulations, we analyzed the center of mass distances between helices B and C within cNTnC (COMdist BC), as summarized in Table 2. Results indicate the averaged COMdist BC for the last 25 ns from multiple runs of simulations increased about 1.6 Å for I61Q, ~0.33 Å greater than for the WT (1.27±0.35 Å).

This greater B-C helices separation suggests there may be changes in the surface structure of the I61Q NcTnC in the region that interacts with the cTnI switch peptide (see next section).

Effects of cTnC (L57Q) and cTnC(I61Q) on the contacts between helices B and C of cNTnC

Contacts between helices B and C were further analyzed to determine how intra-molecular interactions were disrupted by the L57Q or I61Q variants of cTnC. A contact between a pair of residues was defined on the basis of whether any one of the atoms in the first residue was below a set cutoff distance (see Methods section) to atoms in the next residue (32). The percentage of time in contact of each pair was calculated by taking the percentage of structures in which two specified residues were in contact over the 70ns simulation period. In the WT simulation, the following residue pairs between helices B and C were in contact during more than 30% of the total simulation time: L41-L57, L41-M60, L41-I61, G42-L57, M45-L57, and M45-M60. These residues are all hydrophobic residues and contribute to the major interactions between helices B and C (Figure 6). For L57Q, the results averaged over multiple simulations suggest that the percentage of time in contact between residues M45 and Q57 decreased by ~ 26% compared to WT. For I61Q there was much more disruption, with the contact times between all the pairs being generally decreased (L41 – L57 ↓6%; L41 – M60 ↓ 9%; L41 – Q61↓ 15%; G42 – L57 ↓17%, M45 – L57 ↓2%, and M45 – M60 ↓10%) compared to WT. As such, the I61Q variant caused a decrease in hydrophobic interactions between helices B and C. Furthermore, as residues L41, L57, and M60 are known to contribute to the formation of the hydrophobic patch (19), it is possible that the disruption of the hydrophobic interactions introduced by I61Q, and to a lesser extent byL57Q affected the interaction between cNTnC and $cTnI_{147\text{-}163}$. Fig. 5 demonstrates the greater distance between B and C helices for I61Q vs. WT NcTnC (at the 70 ns time point), suggestive of more distributed hydrophobic area, while Fig. 6 demonstrates an increased distance between the B and C helices contact pairs named above for L57Q and especially I61Q. Combined, these data suggest a structural explanation for the experimental observations of reduced cTnI affinity for cTnC that we described in the solution studies (Fig. 3).

Effects of I61Q and L57Q substitutions on the Ca^{2+} binding loop

Residue 61 is at the end of helix C and close to the beginning of the site II Ca^{2+} binding loop. The contacts between residue 61 and residues on the loop (V64, D65, E66, D67, G68, S69, G70, T71, V72, D73 to F74) were monitored and screened. The results indicated that the side chain of Q61 could form hydrogen bonds with these residues. As summarized in Table 3, I61Q formed a backbone hydrogen bond with residue G70 on the Ca^{2+} binding loop ~14% of the simulation time (Figure 7). Moreover, the percentage of time a hydrogen bond was formed between residue 61 and D65 decreased from 74.1±9.2 % to 34.3±15.4 % due to the I61Q substitution. It was reduced even further for L57Q, to only 16.9±12.0 %. Additionally, for L57Q and I61Q, there is less hydrogen bonding occurring overall during the simulation (e.g. 54.5% for I61Q, versus 78.2% for WT).These results suggest that the reason for the experimentally observed decrease in Ca^{2+} binding affinity for the I61Q and L57Q variants may be due to the destabilization of the Ca^{2+} binding loop by formation of hydrogen bond interactions between the variant residues and those in the binding loop.

In comparison, Lim et al. (2008) studied the effect of the D75Y mutation identified in a patient with dilated cardiomyopathy (6). D75 is in the site II Ca^{2+} binding loop (pocket) and they reported, using MD simulations that concerted motion in the pocket was reduced with the D75Y mutation. They also reported a new contact between Y75 and V9 in the N loop of NcTnC. While these MD simulations were done in the absence of Ca^{2+} and for only 6 ns, a common feature between their studies and our is formation of new molecular bonds between amino acids in the Ca2+ binding pocket and others in N-terminal helices. Thus, it will be interesting to see if this is a common feature for all cTnC mutations that result in reduced

Ca^{2+} binding affinity, whether or not they have been associated with cardiomyopathies. As we discussed in our previous study for L48Q cTnC variant which shows a more stable opening conformation and tighter binding with the switch region of cTnI, and we show that L48Q mutation increases the mobility of helix B that facilitates and stabilizes the opening of cNTnC so that it increases the interaction between cNTnC and the switch region of cTnI. We suspect that this effect might stabilize the Ca^{2+} binding loop (the region between helix B and C) that leads to increased Ca2+ binding affinity for L48Q. For L57Q and I61Q in this work, they locate on C helix, differently from L48Q (on B helix). For I61Q, as could be seen from Figure 4B, residue Q61 is very close to the Ca^{2+} binding loop region. According to the MD simulation results, it interrupts the Ca^{2+} binding loop by forming new hydrogen bond and other intramolecular interactions within the loop region, directly disrupting the Ca^{2+} binding. For the interaction with cTnI, MD simulation for I61Q also reveals that helices B and C tend to move away from each other, which interrupts key interactions between the hydrophobic residues in helices B and C. These hydrophobic residues are essential for the formation of the hydrophobic patch where the switch region of cTnI binds to. This might explain the decreased binding affinity of cTnI to cTnC (I61Q) that we observed experimentally.

CONCLUSIONS

In summary, we have characterized the structure and function of cTnC variants L57Q and I61Q with a progressive decrease in Ca^{2+} binding affinity. This was associated with an increased Ca^{2+} dissociation rate in both whole cTn complex and reconstituted thin filament studies(15). The L57Q variant was intermediate between WT and I61Q cTnC and also did not alter cTnC-cTnI interaction in the absence of Ca^{2+}, while it was reduced in the presence of Ca^{2+}. In contrast, I61Q decreased the cTnC-cTnI interaction in both the absence and presence of Ca^{2+}. This difference in the absence of Ca^{2+} suggests a greater structural change in cNTnC may occur with the I61Q mutation than the L57Q mutation. MD simulations revealed that the decreased Ca^{2+} binding induced by I61Q might be due to destabilization of the Ca^{2+} binding site through interruption of intra-molecular interactions when residue 61 forms new hydrogen bonds with G70 on the Ca^{2+} binding loop. Furthermore, the experimentally observed reduction of cTnC-cTnI interaction caused by L57Q or I61Q is likely due to the disruption of key hydrophobic interactions between helices B and C in cNTnC. Our study provides a molecular basis of how single mutations in the C helix of cTnC can reduce Ca^{2+} binding affinity and cTnC-cTnI interaction, which may provide useful insights for a better understanding of molecular alterations in proteins that are involved in cardiomyopathies and thus targets for future gene-based therapies.

Supplementary Material

Refer to Web version on PubMed Central for supplementary material.

Acknowledgments

Computer time through the DOE Office of Biological Research was provided by the National Energy Research Scientific Computing Center, which is supported by the Office of Science of the U.S. Department of Energy under contract No.DE-AC02-05CH11231 (to V.D). DW is the recipient of the pre-doctoral fellowship from the American Heart Association. MEM acknowledges support by a grant from the Department of Defense through the National Defense Science and Engineering Graduate Fellowship Program for the MD studies. MR is an Established Investigator of the American Heart Association and acknowledges support from the National Institutes of Health, R01 HL65497 and. VD is grateful for support for the computational studies from the National Institutes of Health, R01GM50789.

Abbreviations

cTnC	intact cardiac troponin C
cNTnC	N-domain of cTnC
cTn	cardiac whole troponin
cTnC(L57Q)	intact cTnC variant with the Leu57Gln mutation
cTnC(I61Q)	intact cTnC variant with the Ile61Gln mutation
cTnI	cardiac troponin I
cTnI147-163	cTnI peptide corresponding to residues 147-163
IANBD	N-(2-(iodoacetoxy)ethyl)-N-methyl)amino-7-nitrobenz-2-oxa-1,3-diozole
MD	molecular dynamics
WT	wild-type
PDB	Protein Data Bank
Cα-RMSD	root-mean-square deviation of Cα atom coordinates from the starting structure
COMdist	distances between the center of mass of two objects

REFERENCES

1. Gordon AM, Homsher E, Regnier M. Regulation of contraction in striated muscle. Physiol. Rev. 2000; 80:853–924. [PubMed: 10747208]
2. Maytum R, Lehrer SS, Geeves MA. Cooperativity and switching within the three-state model of muscle regulation. Biochemistry. 1999; 38:1102–1110. [PubMed: 9894007]
3. Rarick HM, Tu XH, Solaro RJ, Martin AF. The C terminus of cardiac troponin I is essential for full inhibitory activity and Ca2+ sensitivity of rat myofibrils. J. Biol. Chem. 1997; 272:26887–26892. [PubMed: 9341121]
4. Willott RH, Gomes AV, Chang AN, Parvatiyar MS, Pinto JR, Potter JD. Mutations in Troponin that cause HCM, DCM AND RCM: what can we learn about thin filament function? J Mol Cell Cardiol. 2010; 48:882–892. [PubMed: 19914256]
5. Tardiff JC. Thin filament mutations: developing an integrative approach to a complex disorder. Circ Res. 2011; 108:765–782. [PubMed: 21415410]
6. Lim CC, Yang H, Yang M, Wang CK, Shi J, Berg EA, Pimentel DR, Gwathmey JK, Hajjar RJ, Helmes M, Costello CE, Huo S, Liao R. A novel mutant cardiac troponin C disrupts molecular motions critical for calcium binding affinity and cardiomyocyte contractility. Biophys J. 2008; 94:3577–3589. [PubMed: 18212018]
7. Robinson P, Mirza M, Knott A, Abdulrazzak H, Willott R, Marston S, Watkins H, Redwood C. Alterations in thin filament regulation induced by a human cardiac troponin T mutant that causes dilated cardiomyopathy are distinct from those induced by troponin T mutants that cause hypertrophic cardiomyopathy. J Biol Chem. 2002; 277:40710–40716. [PubMed: 12186860]
8. Mirza M, Marston S, Willott R, Ashley C, Mogensen J, McKenna W, Robinson P, Redwood C, Watkins H. Dilated cardiomyopathy mutations in three thin filament regulatory proteins result in a common functional phenotype. J Biol Chem. 2005; 280:28498–28506. [PubMed: 15923195]
9. Tikunova SB, Liu B, Swindle N, Little SC, Gomes AV, Swartz DR, Davis JP. Effect of calcium-sensitizing mutations on calcium binding and exchange with troponin C in increasingly complex biochemical systems. Biochemistry. 2010; 49:1975–1984. [PubMed: 20128626]
10. Davis JP, Rall JA, Alionte C, Tikunova SB. Mutations of Hydrophobic Residues in the N-terminal Domain of Troponin C Affect Calcium Binding and Exchange with the Troponin C-Troponin

I96-148 Complex and Muscle Force Production. Journal of Biological Chemistry. 2004; 279:17348–17360. [PubMed: 14970231]

11. Tikunova SB, Rall JA, Davis JP. Effect of hydrophobic residue substitutions with glutamine on Ca(2+) binding and exchange with the N-domain of troponin C. Biochemistry. 2002; 41:6697–6705. [PubMed: 12022873]
12. Kekenes-Huskey PM, Lindert S, McCammon JA. Molecular Basis of Calcium-Sensitizing and Desensitizing Mutations of the Human Cardiac Troponin C Regulatory Domain: A Multi-Scale Simulation Study. PLoS Comput Biol. 2012; 8:e1002777. [PubMed: 23209387]
13. Wang D, Robertson IM, Li MX, McCully ME, Crane ML, Luo Z, Tu A-Y, Daggett V, Sykes BD, Regnier M. Structural and Functional Consequences of the Cardiac Troponin C L48Q Ca2+-Sensitizing Mutation. Biochemistry. 2012; 51:4473–4487. [PubMed: 22591429]
14. Parvatiyar MS, Pinto JR, Liang J, Potter JD. Predicting cardiomyopathic phenotypes by altering Ca2+ affinity of cardiac troponin C. J. Biol. Chem. 2010; 285:27785–27797. [PubMed: 20566645]
15. Kreutziger KL, Piroddi N, McMichael JT, Tesi C, Poggesi C, Regnier M. Calcium binding kinetics of troponin C strongly modulate cooperative activation and tension kinetics in cardiac muscle. J Mol Cell Cardiol. 2011; 50:165–174. [PubMed: 21035455]
16. Dong WJ, Rosenfeld SS, Wang CK, Gordon AM, Cheung HC. Kinetic studies of calcium binding to the regulatory site of troponin C from cardiac muscle. J. Biol. Chem. 1996; 271:688–694. [PubMed: 8557674]
17. Martyn DA, Regnier M, Xu D, Gordon AM. Ca2+ - and cross-bridge-dependent changes in N- and C-terminal structure of troponin C in rat cardiac muscle. Biophys. J. 2001; 80:360–370. [PubMed: 11159408]
18. Dong WJ, Robinson JM, Stagg S, Xing J, Cheung HC. Ca2+-induced conformational transition in the inhibitory and regulatory regions of cardiac troponin I. J Biol Chem. 2003; 278:8686–8692. [PubMed: 12511564]
19. Wang D, Robertson IM, Li MX, McCully ME, Crane ML, Luo Z, Tu AY, Daggett V, Sykes BD, Regnier M. Structural and Functional Consequences of the Cardiac Troponin C L48Q Ca(2+)-Sensitizing Mutation. Biochemistry. 2012
20. Patton C, Thompson S, Epel D. Some precautions in using chelators to buffer metals in biological solutions. Cell Calcium. 2004; 35:427–431. [PubMed: 15003852]
21. George SE, Su Z, Fan D, Wang S, Johnson JD. The Fourth EF-Hand of Calmodulin and Its Helix-Loop-Helix Components: Impact on Calcium Binding and Enzyme Activation†. Biochemistry. 1996; 35:8307–8313. [PubMed: 8679587]
22. Kreutziger KL, Gillis TE, Davis JP, Tikunova SB, Regnier M. Influence of enhanced troponin C Ca2+-binding affinity on cooperative thin filament activation in rabbit skeletal muscle. J Physiol. 2007; 583:337–350. [PubMed: 17584846]
23. Beck, DAC.; McCully, ME.; Alonso, DOV.; Daggett, V. ilmm. 2000-2012. in lucem molecular mechanics.
24. Levitt M, Hirshberg M, Sharon R, Daggett V. Potential-energy function and parameters for simulations of the molecular-dynamics of proteins and nucleic-acids in solution. Comput. Phys. Commun. 1995; 91:215–231.
25. Li MX, Spyracopoulos L, Sykes BD. Binding of cardiac troponin-I147-163 induces a structural opening in human cardiac tropoin-C. Biochemistry. 1999; 38:8289–8298. [PubMed: 10387074]
26. Pettersen EF, Goddard TD, Huang CC, Couch GS, Greenblatt DM, Meng EC, Ferrin TE. UCSF chimera - A visualization system for exploratory research and analysis. J. Comput. Chem. 2004; 25:1605–1612. [PubMed: 15264254]
27. Levitt M, Hirshberg M, Sharon R, Laidig KE, Daggett V. Calibration and testing of a water model for simulation of the molecular dynamics of proteins and nucleic acids in solution. J. Phys. Chem. B. 1997; 101:5051–5061.
28. Kell GS. Precise Representation of Volume Properties of Water at 1 Atmosphere. J. Chem. Eng. Data. 1967; 12:66–69.
29. Sopkova J, Renouard M, Lewit-Bentley A. The crystal structure of a new high-calcium form of annexin V. J Mol Biol. 1993; 234:816–825. [PubMed: 8254674]

30. Kruger M, Zittrich S, Redwood C, Blaudeck N, James J, Robbins J, Pfitzer G, Stehle R. Effects of the mutation R145G in human cardiac troponin I on the kinetics of the contraction-relaxation cycle in isolated cardiac myofibrils. J Physiol. 2005; 564:347–357. [PubMed: 15718266]

31. Dong WJ, Xing J, Ouyang Y, An J, Cheung HC. Structural kinetics of cardiac troponin C mutants linked to familial hypertrophic and dilated cardiomyopathy in troponin complexes. J Biol Chem. 2008; 283:3424–3432. [PubMed: 18063575]

32. McCully ME, Beck DA, Daggett V. Microscopic reversibility of protein folding in molecular dynamics simulations of the engrailed homeodomain. Biochemistry. 2008; 47:7079–7089. [PubMed: 18553935]

Highlights

- Study of L57Q and I61Q cTnC using solution and *in silico* techniques is presented.
- Solution studies indicate both variants decrease the Ca^{2+} binding affinity to cTnC.
- Both variants reduced cTnI affinity to cTnC in Ca^{2+} saturated states.
- MD simulation shows disruption between helices B/C by both cTnC variants.
- cTnC (I61Q) formed hydrogen bonds with the residues on the Ca^{2+} binding loop.

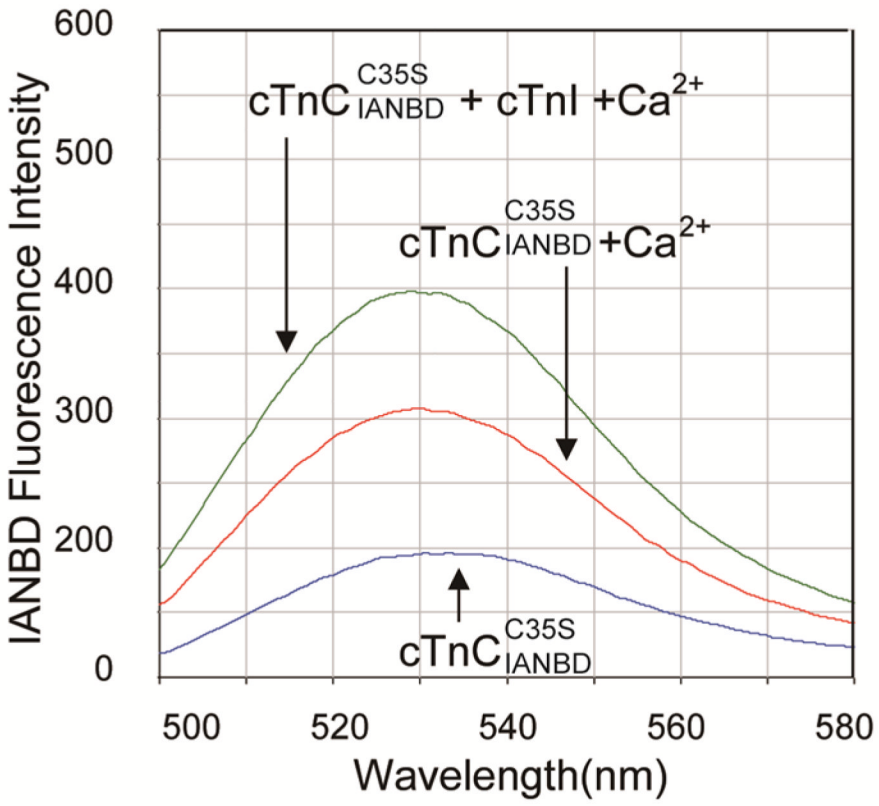

FIGURE 1.

Representatives of the IANBD emission spectra of the IANBD (blue), $\mathrm{IANBD} \bullet \mathrm{Ca}^{2+}$ (red) and $\mathrm{IANBD} \bullet \mathrm{Ca}^{2+} \bullet \mathrm{cTnI}$ (green).

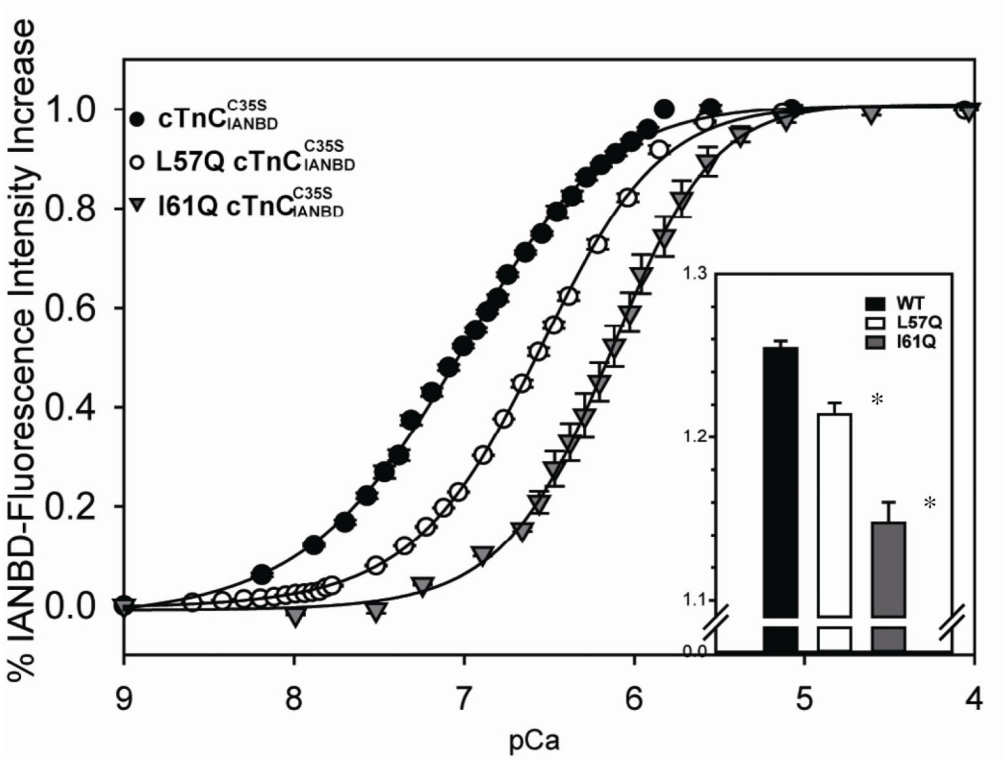

FIGURE 2.

Effects of L57Q and I61Q cTnC on the Ca^{2+} dependent changes in the fluorescence of IANBD complexes. (●) Ca^{2+} binding to IANBD; (○) Ca^{2+} binding to L57Q IANBD; (▼) Ca^{2+} binding to IANBD. Inset graph: the magnitude of IANBD fluorescence increase of IANBD and other variants. The error bars represent the standard error of 3-5 experiments. $P<0.05$ as compared to control protein.

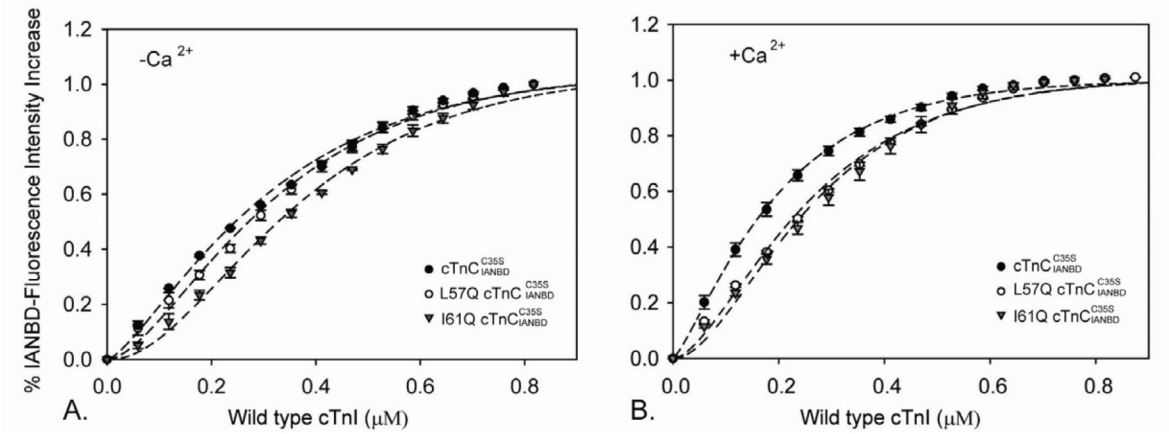

FIGURE 3.

Effects of L57Q and I61Q cTnC on the binding of cTnI to $_{\text{IANBD}}$. The binding was determined by measuring the changes in IANBD fluorescence emission intensity of $_{\text{IANBD}}$ titrating with cTnI in (A) the absence of Ca^{2+} and (B) the presence of Ca^{2+}.(●) $_{\text{IANBD}}$, (○) $_{\text{IANBD}}$, (▼) $_{\text{IANBD}}$. The error bars represent the standard error of 3-5 experiments. $P<0.05$ as compared to control protein.

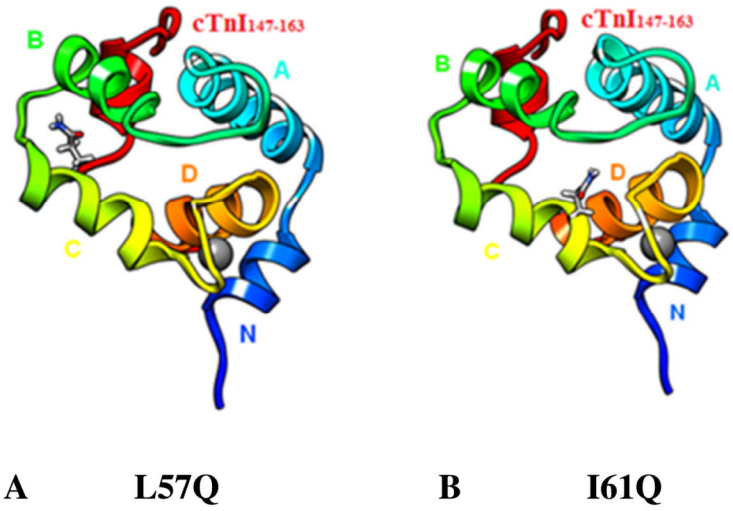

FIGURE 4.

Positions of mutated residues in the cNTnC•Ca^{2+} •$cTnI_{147-163}$ structure. (A) L57Q on helix-C; (B) I61Q on helix-C. cNTnC: Helix-N (blue 4-10), Helix-A(cyan 14-28), Helix-B(green 41-48), Helix-C(yellow 54-64), Helix-D (orange 74-82), $cTnI_{147-163}$(red) and Ca^{2+} (grey).

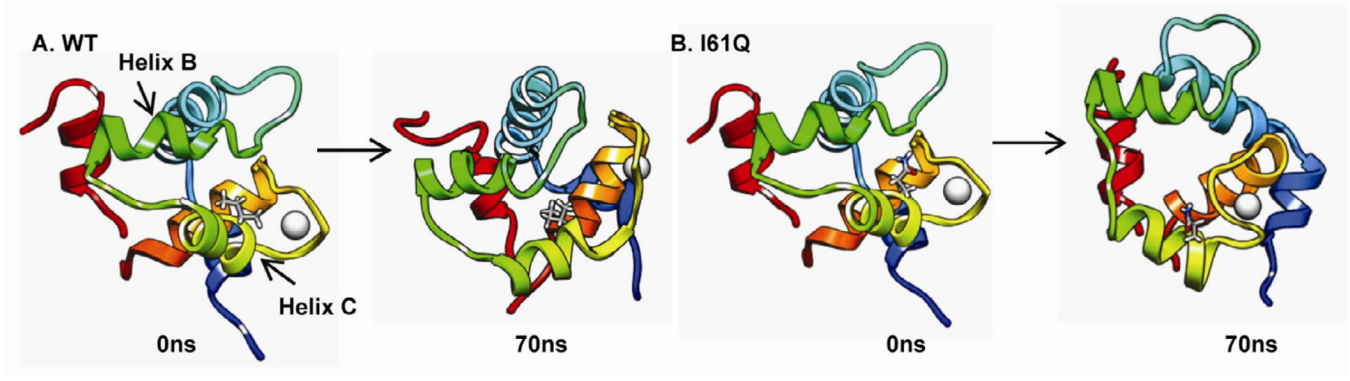

FIGURE 5.
Snapshots from simulations showing motion between helix B and C at 0ns and 70ns. ((A) WT; (B) I61Q)

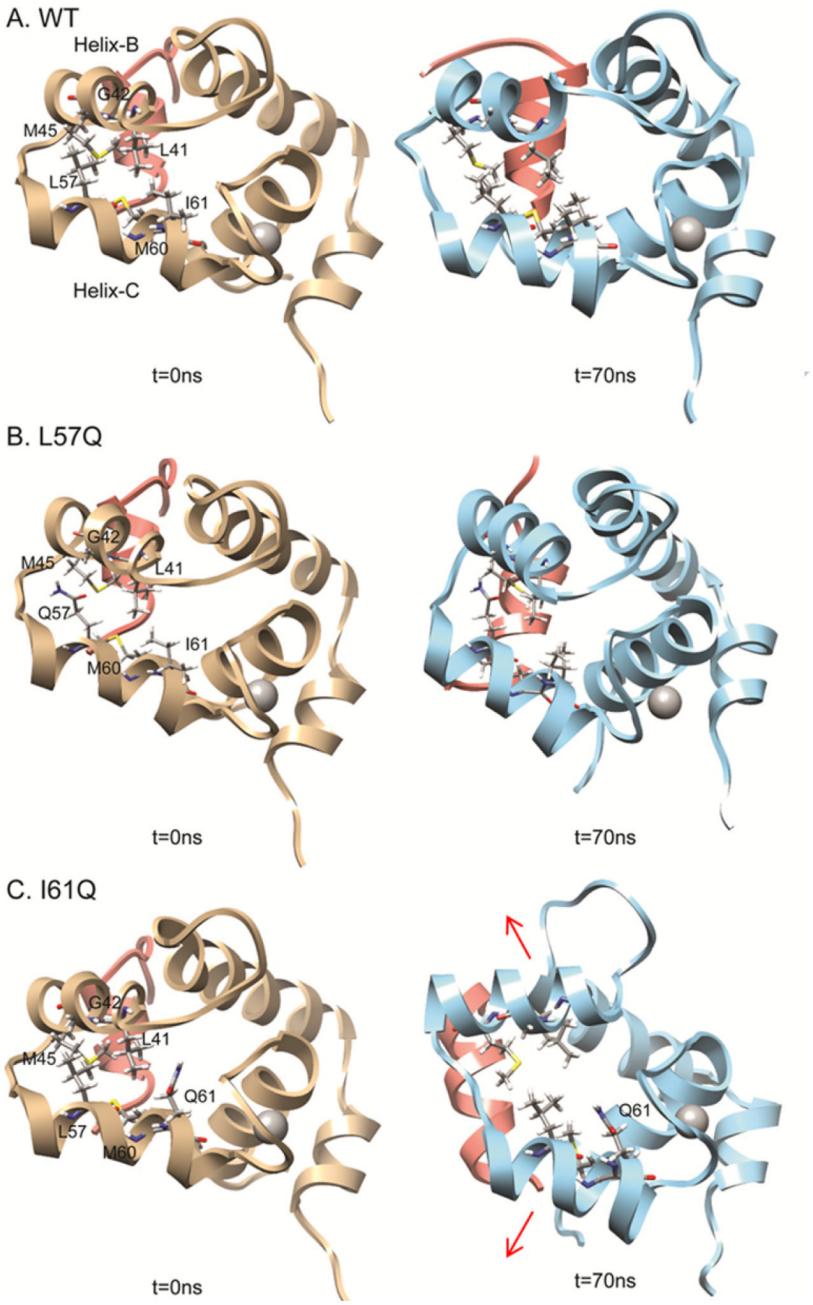

FIGURE 6.

Disruption of cTnC variants I61Q and L57Q on the interactions between helices B (residues 41-48) and C (residues 54-64) of cNTnC. WT (shown in panel A) simulations results suggest that the following residues pairs between helices B and C were in contact during more than 30% of the total simulation time: L41 *vs.* L57, L41 *vs.* M60, L41 *vs.* I61, G42 *vs.* L57, M45 *vs.* L57, and M45 *vs.* M60. For L57Q (shown in panel B), contact time between M45 and Q57 was decreased for 26% compared to WT; For I61Q (shown in panel C), contact time between all the pairs listed above were decreased (L41 *vs.* L57 ↓6%; L41 *vs.*

M60 ↓ 9%; L41 *vs.* Q61↓ 15%; G42 *vs.* L57 ↓17%, M45 *vs.* L57↓2%, and M45 *vs.* M60 ↓10%.) compared to WT.

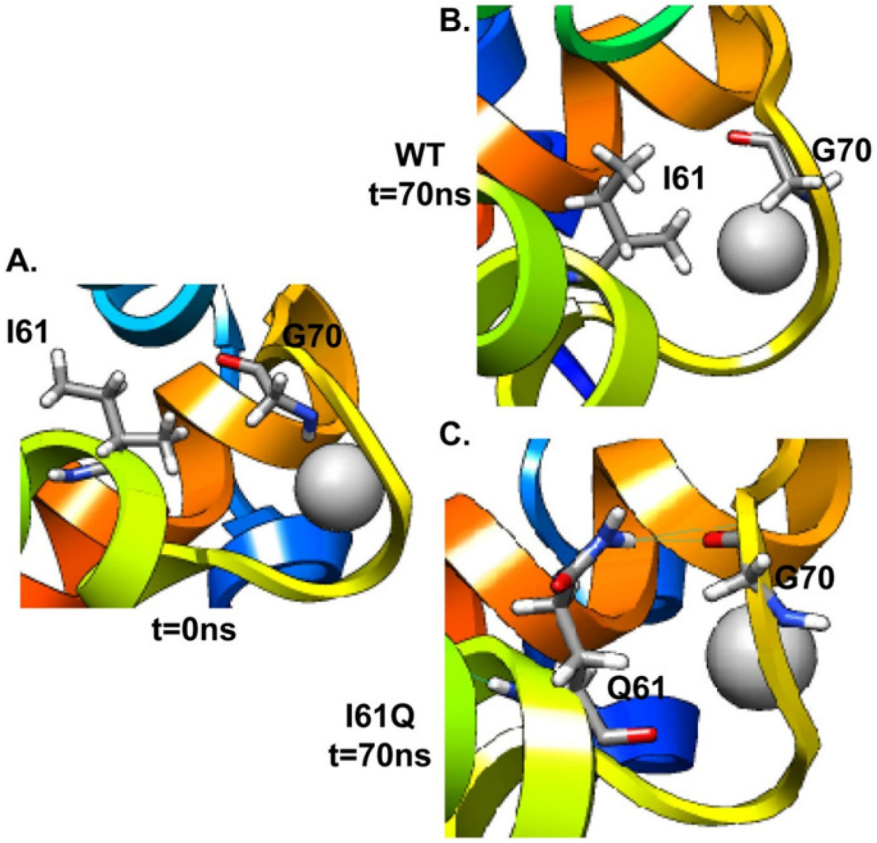

FIGURE 7.
Snapshots from I61Q and WT simulations for Ca^{2+} binding site II at 0ns (A) and 70ns ((B) WT; (C) I61Q).

Table 1

Summary of Ca^{2+} dissociation rate (k_{off}) from cTnC in whole cTn complex or in reconstituted thin filaments by stopped-flow spectroscopy with Quin-2 fluorescence at 15°C.

	cTn Complex[a] Ca^{2+} k_{off} (s^{-1})	Thin filament[†] Ca^{2+} k_{off} (s^{-1})
WT[#]	29.7±0.5	75.4± 4.8
L57Q	51.8±2.1[*]	74.1± 11.6
I61Q(15)[#]	67.0±9.3	237.7 ± 30.5

[a] Tn complexes (6 uM) +100 uM Quin-2)

[†] Thin Filament (5.4 uM cTn, 42 uM skel Actin, 6 uM Tm) +100 uM Quin-2)

[#] WT and I61Q data reported by Kreutziger *et al.* (15), cited here for comparison with L57Q

[*] cTnC. $P < 0.05$

Table 2

Summary of distances (Å) between the center of mass of helices B and C.

	Avg. Comdist in NMR ensembles	Avg. Comdist in starting structures	Comdist BC helices (45-70ns)	ΔComdist BC helices*
WT	13.73 ± 0.29	13.57 ± 0.00	14.71 ± 0.29	1.27 ± 0.35
L57Q	-	13.50 ± 0.02	14.60 ± 0.32	1.48 ± 0.35
I61Q	-	13.57 ± 0.02	15.24 ± 0.26	1.60 ± 0.30

*ΔComdist BC helices= Avg.Comdist (45-70ns)−Avg.Comdist at 0ns

Table 3

Percentage of time hydrogen bond was formed between residue 61 and residues in Ca^{2+} binding loop

	WT	L57Q	I61Q
V64	4.1 ± 1.2 %	5.8 ± 0.02 %	2.2 ± 1.0 %
D65	74.1 ± 9.2 %	16.9 ± 12.0 %	34.3 ± 15.4 %
S69	-	-	3.7 ± 2.8 %
G70	-	-	14.0 ± 6.2 %
T71	-	-	0.3 ± 0.1%